

# Casimir Force on a Light Front

S.S. Chabysheva,<sup>1</sup> J.R. Hiller<sup>1,2</sup>

<sup>1</sup>Department of Physics, University of Idaho, Moscow, ID 83843 USA

<sup>2</sup>Department of Physics and Astronomy,  
University of Minnesota-Duluth, Duluth, MN 55812 USA

August 19, 2020

## Abstract

Depending on the point of view, the Casimir force arises from variation in the energy of the quantum vacuum as boundary conditions are altered or as an interaction between atoms in the materials that form these boundary conditions. Standard analyses of such configurations are usually done in terms of ordinary, equal-time (Minkowski) coordinates. However, physics is independent of the coordinate choice, and an analysis based on light-front coordinates, where  $x^+ \equiv t + z/c$  plays the role of time, is equally valid. After a brief historical introduction, we illustrate and compare equal-time and light-front calculations of the Casimir force.

## 1 Introduction

The archetype of the Casimir force [1, 2, 3, 4, 5, 6, 7, 8, 9] is the interaction between two closely spaced parallel conducting plates. A loose argument for the force is that the plates restrict the number of permitted electromagnetic modes between the plates while the space outside enjoys the full range; the difference in zero-point energy densities causes an inward pressure. Though intuitive, the argument fails in other situations and is actually misleading, because both densities are infinite and require regularization. For example, the same argument would imply that a conducting spherical shell would experience a collapsing, inward force, but this is not the case.<sup>1</sup>

Standard analyses of such configurations are usually done in terms of ordinary, equal-time (Minkowski) coordinates. However, physics is independent of the coordinate choice, and an analysis based on light-front coordinates [12, 13, 14, 15, 16, 17, 18], where  $x^+ \equiv t + z/c$  plays the role of time, is equally valid. This review provides a survey of applications of light-front coordinates to the Casimir force [19, 20, 21, 22] and compares the results with equal-time calculations for a massless scalar field with boundaries fixed by parallel plates. Extensions to other fields, such as photons, is straightforward. The primary complication that arises for light-front calculations is for plates perpendicular to the longitudinal direction, for which the exact nature of the boundary conditions relative to the light-front space and time coordinates is critical.

The electromagnetic Casimir effect can also be described in terms of the van der Waals interaction between the atoms in the boundary materials. However, the effect can occur in principle for any quantum

---

<sup>1</sup>There was an attempt to balance this supposed inward force by the outward repulsion of the electron's charge density and arrive at a mechanical model of the electron [10, 11].

field, while the van der Waals force is limited to electromagnetic interactions. The only question is how to select appropriate boundary conditions for the particular field. Implicit in the boundary conditions will be a force, analogous to the van der Waals force, between the elements of the materials forming the boundaries.

The reality of the vacuum energy is supported by a demonstration that the inertial and gravitational masses of Casimir energy are proportional [23], consistent with the general relativistic equivalence principle. However, the interpretation that the Casimir effect provides proof that vacuum energies are real has been questioned [24]. Because the Casimir force can in principle be computed from the van der Waals force between atoms in the material forming the boundaries, the vacuum energy does not need to be invoked to explain the Casimir force. However, from the point of view of assembling a configuration that gives rise to a measurable Casimir force, one can compute the work done during an adiabatic assembly and translate that into a potential energy, the gradient of which determines the force acting between the assembled parts. One would normally consider this potential energy to be stored in a rearrangement of the electromagnetic field, which in the case of the Casimir effect, would be vacuum modes. An analogy is the energy stored in a configuration of two charges, brought together against the Coulomb force between them; this energy is associated with the energy of the electrostatic field minus the self energies. The two views are complementary.

Vacuum effects such as the Casimir force and Casimir torque will be important for the design of nanoscale devices. The interatomic forces can create surface adhesion effects that can even break such devices. Conversely, the effects can be incorporated to improve sensitivity of accelerometers and torsion sensors [25].

The remainder of this paper contains a brief historical overview in Sec. 2, followed by specific calculations of the Casimir force between parallel plates in Sec. 3. The calculations compare use of light-front coordinates with that of equal-time coordinates for the case of a massless scalar field subject to either periodic boundary conditions or zero boundary conditions at the plates. For the light-front case, plates are considered both parallel and perpendicular to the longitudinal direction. A summary is included as Sec. 4.

## 2 Historical background

### 2.1 Precursors

In classical physics, one can obtain an attractive  $1/r^6$  potential between polarizable objects a distance  $r$  apart. This is driven by thermal fluctuations that induce a dipole moment in one object which in turn induces a dipole moment in the other. The effect is linear in the temperature  $T$ . This is contradicted by quantum mechanics where the effect is constant at low  $T$  and vacuum fluctuations play the role of the thermal fluctuations.

The original proposal by van der Waals for an attractive force between molecules was associated with a Yukawa type potential  $-A\frac{e^{-Br}}{r}$  that was to explain the pressure term in the equation of state

$$(P + \frac{a}{V^2})(V - b) = nRT. \quad (1)$$

It was London who obtained the correct form for short distances [26]

$$V = -\frac{3\hbar\omega_0\alpha^2}{4r^6} \quad (2)$$

from fourth-order perturbation theory, with  $\omega_0$  the characteristic transition frequency for transitions to excited states and  $\alpha$  is the static polarizability.

Casimir and Polder improved on this result for larger distances where  $\omega_0 r/c$  is much greater than unity and retardation becomes important. The London result is then modified to [27]

$$V = -\frac{23\hbar c}{4\pi r^7}\alpha_A\alpha_B \quad (3)$$

for a pair of atoms with polarizabilities of  $\alpha_X$ . This result was initially computed by two-photon exchange in perturbation theory but is consistent with polarizations induced by vacuum fluctuations [28].

In 1947, Lamb and Retherford measured the  $2S_{1/2}$ - $2P_{1/2}$  split in atomic levels [29]. This is usually calculated as a perturbation due to virtual photon exchange [30]. However, as early as 1948, Welton interpreted the energy shift as a consequence of interaction with the vacuum fluctuations of the electromagnetic field [31]. The vacuum field fluctuations induce fluctuations in the electron position, essentially a Stark effect driven by the vacuum field, which cause corrections to the Coulomb potential; these corrections result in the Lamb shift. It was also suggested by Feynman that the Lamb shift could be considered as a change in the zero-point field energy due to the presence of atoms [32]. The Lamb shift is also modified by the presence of a nearby surface, which alters the available photon modes.

The relationship between fluctuation and dissipation is such that if a system can dissipate energy to its surrounding reservoir irreversibly, then the reservoir must induce fluctuations in the system. Thus radiation reaction implies the existence of a vacuum field. Consequently, the spectral density of the vacuum field must be directly related to the form of the radiation reaction. Because the radiation reaction is proportional to the third derivative of the position, the spectral energy density of the vacuum is proportional to the third power of the frequency [33, 34]. Dissipation due to radiation reaction will act to exponentially damp the position which would drive the fundamental commutator  $[x, p]$  of position and momentum to zero; noncommutativity is preserved by the fluctuations of the vacuum.

The concept of zero-point energy began with Planck in 1912, with his “second” theory of blackbody radiation. Heisenberg developed the concept in connection with a quantum harmonic oscillator. From a more modern, field-theoretic viewpoint, the electric and magnetic field operators do not commute, and, therefore, they cannot both be determined simultaneously. Consequently, the energy of the electromagnetic state, which has contributions from both fields, can never be zero. Zero-point fluctuations in crystals do scatter light at zero temperature, so much so that for helium that it cannot crystallize and x-ray diffraction is impacted in ordinary crystals. A shift in energy, to remove the zero-point energy from the Hamiltonian, does not eliminate vacuum effects. In particular, the expectation values for the momentum squared and position squared remain nonzero in the vacuum and fluctuations in momentum and position remain.

W. Pauli rejected the notion of zero-point energy, saying “it does not create any gravitational field, as is known from experience” [35]. This is to be contrasted with the more recent puzzle, that the contribution of zero-point energy to the cosmological constant is too large by 120 orders of magnitude [36]. Such contradictions aside, the Casimir effect can play a role in the structure of space-time. It can provide a source for compactification of extra dimensions [37] and, more generally, it can factor into the vacuum energy of space-times that are not flat [38]. Measurements of the local vacuum energy density could then, in principle, constrain the global topology of the Universe.

## 2.2 Casimir effect

The attractive force between two conducting plates was first calculated by Casimir in 1948 [1]. He was apparently not familiar with the work of Lamb or Welton but was instead motivated by a remark by Bohr about zero-point energy. The original Casimir-effect paper cites his own work on the retarded van der Waals interaction that included zero-point fluctuations. An alternate derivation, based on interactions of the charges in the plates rather than the vacuum energy, has been given by Schwinger, DeRaad and Milton [39].

The basic result is that, for parallel plates separated by a distance  $a$  with surface area  $A$ , the leading  $a$ -dependent contribution to the vacuum energy between the plates is

$$E_0(a) = -\frac{\pi^2 \hbar c A}{720 a^3}. \quad (4)$$

The construction requires regularization of the sum over zero-point modes but is independent of the regularization. Terms independent of  $a$  are subtracted as self-energies associated with individual plates. The Casimir force per unit area is then

$$P = -\frac{1}{A} \frac{dE_0}{da} = -\frac{\pi^2 \hbar c}{240 a^4}. \quad (5)$$

The presence of  $\hbar$  in both the energy and the force shows this to be a quantum effect. Typical magnitudes are  $P = 10^5$  Pa for  $a = 10$  nm and  $P = 10^{-3}$  Pa for  $a = 1$   $\mu$ m.

Calculations of the Casimir effect usually rely on separation of variables in the wave equation to obtain the eigenspectrum, which requires simple symmetric geometries for boundaries. The result for parallel plates can be obtained as a limit of a calculation for a wedge [4].

Instead of impenetrable walls with boundary conditions of zero, periodic boundary conditions can also be considered. For a massless scalar field in one space dimension with periodicity  $a$ , the energy density is  $-\pi/6a^2$ , to be compared with  $-\pi/24a^2$  for impenetrable walls separated by  $a$ .

Casimir's result was extended to realistic materials by Lifshitz, who derived the Casimir force between plates with complex dielectric permittivity  $\epsilon(\omega)$  [40]. Casimir's result is recovered in the limit of  $\epsilon \rightarrow \infty$ . The determination requires consideration of the interior of the media as well as the gap between. The interactions are not additive, because of screening effects that weaken the van der Waals interactions between individual atoms. The Casimir energy and force are then most conveniently given in terms of the permittivity and permeability of the media. An alternative is to represent the media effects through an impedance at the boundary. The treatment of the media is justified by the Ewald-Oseen extinction theorem [41], which limits significant field penetration to approximately one wavelength. The  $a^{-4}$  power-law behavior remains, but the coefficient is different. The screening effect can be neglected only if the media are dilute. Penetrable walls can be modeled with delta functions [24].

Because a calculation based on the van der Waals force shows that the Casimir force is dependent on the magnitude of the fine-structure constant  $\alpha$ , there is also criticism [24] of the standard Casimir result for being independent of  $\alpha$ . It is obtained from more sophisticated calculations only in the limit of infinite  $\alpha$ . However, the standard result is derived for perfectly conducting surfaces, which is equivalent to taking an infinite value for  $\alpha$  from the beginning of the calculation; the boundary conditions correspond to the zero skin depth associated with infinite conductivity, and  $\alpha$  is proportional to the conductivity [42].

Other geometries and materials can result in a cutoff dependence which reflects the physical properties of the materials at high frequencies. For conducting plates, the surfaces become effectively transparent at high frequencies; however, the dominant contribution to the Casimir force comes from frequencies well below this cutoff.

For a spherical conducting shell of radius  $a$ , Boyer obtained a Casimir energy of [11] (See also [39, 43].)

$$E_0(a) = +\frac{0.09 \hbar c}{2a}. \quad (6)$$

This corresponds to a repulsive force that tries to expand the sphere, but a negative result and an attractive force can be obtained if one considers realistic material for the shell [44]. Kenneth and Klick [45] also show that the Casimir force between two dielectrics must be attractive, which applies here because the shell can be cut into two hemispheres which must then attract.

The evaluation for a spherical shell requires some care [4] because of surface divergences that require additional counterterms in the case of a massless scalar field. However, for the electromagnetic field, the inside and outside surface divergences cancel, in the principal-value sense, and one gets a finite result after simply subtracting the free-space density.

When the boundaries are asymmetric or made from materials that are anisotropic, such as a dielectric birefringent crystal, there is a Casimir torque as well as a force. The optical axis with the highest refractive index tries to align, resulting in a torque. A torque measurement has been done recently by Somers and co-workers [46].

### 2.3 *Related phenomena*

Placing an atom in a bounded domain causes energy shifts to depend on the nature of the normal modes for the given boundary conditions and on the position of the atom. This can result in a force between a boundary and the atom. This can include retardation effects that change the dependence on separation  $r$  from  $r^{-3}$  to  $r^{-4}$  as the atom interacts with its image in the conducting plate. Casimir and Polder explained this result in terms of zero-point energy [27]. It can also be obtained by a modification of the Lamb-shift analysis where the virtual photon is subject to the boundary conditions associated with the plate [9]. The spectroscopy of atoms between two spherical mirrors has been considered by Heizen and Feld [47].

The rate of spontaneous emission from an excited atom is modified by the presence of a reflecting surface. This has been verified experimentally by Drexhage [48]. In particular, placement of an atom between two reflecting mirrors can suppress spontaneous emission when the mirror spacing is less than one-half of the wavelength of the light emitted in the transition, because the necessary mode is not available [49, 50, 51]. This has also been observed experimentally [52]. In general, the discrete spectrum of a confined space may not include a mode that resonates with a particular transition frequency.

Spontaneous decay is driven by interaction with the vacuum photon energy density and by radiation reaction due to fields generated by fluctuations in the atomic dipole moment. The interaction with the vacuum photons is analogous to stimulated emission where the atom interacts with thermal photons; however, this interaction accounts for only half of the spontaneous emission rate, with the other half due to radiation reaction. For the ground state, the two effects cancel, and there is no spontaneous absorption.

Magnetic moments are affected by boundary conditions. For example, measurements of the anomalous magnetic moment  $g - 2$  for the electron that use a Penning trap must take into account the consequences of cavity QED, which is to introduce an interaction with the vacuum fields of the cavity. From the point of view of perturbation theory, the photons in loops must occupy states allowed by the cavity, which is a restriction from free-space modes. Welton attempted a derivation of  $g - 2$  based on interactions with the vacuum fields but obtained the wrong sign [31]. This was corrected to include radiation reaction effects that renormalize the mass [53]; however, the result remains cut-off dependent.

The bag model for hadrons [54] includes contributions to the energy from the Casimir effect for interior quarks and gluons, trapped in a spherical “bag.” The effect is about 10% of the mass for a nucleon, despite that fact the the free-space zero-point energy for fermions is negative. The computation of the Casimir energy [55] typically ignores interactions between the quarks and gluons. For the quarks, the boundary conditions cannot be simply the setting the Dirac field to zero; instead a condition is imposed that prevents flux through the boundary. This yields an attractive force for fermions between plates and a repulsive force for a spherical shell [56, 57, 58].

## 2.4 Regularization

In a quantum field theoretic analysis of vacuum effects, the choice of operator ordering can determine whether an effect is due to vacuum fluctuations or radiation reaction or a combination of the two. For spontaneous emission, there is no choice of ordering that will allow for the effect to be purely due to vacuum fluctuations; for standard normal ordering, the rate is determined by radiation reaction, and for antinormal ordering by a combination with vacuum fluctuations [34, 59]. For the Lamb shift, the effect is due to vacuum fluctuations for symmetric ordering, radiation reaction for normal ordering, and a mixture for antinormal ordering [59, 60]. The ordering of creation and annihilation operators does, of course, control vacuum effects to some extent; normal ordering explicitly subtracts them from the Hamiltonian. From this point of view, the Casimir force can be attributed to source fields when normal ordering is used and to vacuum fields when symmetric ordering is used.

Computation of the Casimir force from vacuum energy requires subtraction between two infinite quantities, the vacuum energy in free space and the vacuum energy in the bounded space. The leading divergence of the free vacuum energy is of order  $p^d$ , where  $p$  is the cutoff momentum and  $d$  is the dimension of space-time. However, the free vacuum energy is computed as an integral, and the bounded-space vacuum energy as a sum. The simplest approach, as done originally, is to introduce cutoffs, to be removed after the subtraction. However, cutoff independent methods have been developed, based on Greens functions and on the Abel-Plana formula [61, 4]

$$\sum_{n=0}^{\infty} F(n) - \int_0^{\infty} F(t)dt = \frac{F(0)}{2} + i \int_0^{\infty} dt \frac{F(it) - F(-it)}{e^{2\pi t} - 1}. \quad (7)$$

There are actually two ways to subtract the free-space energy. One is to work with the boundary conditions already in place, and the other is to bring the boundaries in from infinite separation. The second approach is useful when a boundary itself is associated with an infinite energy relative to free space; this energy must be subtracted along with the free-space energy. This happens because there can exist surface divergences in the vacuum energy density that are nonintegrable, making the energy associated with the vicinity of the surface infinite, even for a compact domain. This can be controlled by subtraction, as already mentioned, or by invoking more realistic boundary conditions that do not create the density divergence in the first place.

## 2.5 Measurements

Early tests of the Casimir effect were difficult to do and inconclusive. The first qualitative observation was by Sparnaay in 1958 [62], where the results are described as being “not inconsistent” with the prediction by Casimir. The first quantitative measurement was done by Lamoreaux [63], using a sphere and a plate rather than two plates, to avoid the difficulty associated with maintaining plate alignment; it confirmed the Casimir force (as modified for a spherical surface) for separations between 0.6 and 1  $\mu\text{m}$ . For shorter separations, the Casimir force becomes just the unretarded van der Waals-London force; for larger, thermal effects become important. Subsequently, there were many experiments testing various aspects, including geometry, finite temperature, and material properties. In addition, the direction of the force has been observed to reverse from attractive to repulsive when a dielectric is placed between objects [64]. For a recent citation of experiments and discussion of methods, see [9].

For a list of early experiments intended to confirm the existence of zero-point energies, see [65]. In particular, Mulliken showed in 1924, before Heisenberg’s derivation of zero-point energy, that  $\text{B}_{10}\text{O}_{16}$  and  $\text{B}_{11}\text{O}_{16}$  molecules have a nonzero minimum vibration energy. A much more recent experiment shows evidence of a lower bound on the motion of laser-cooled trapped ions [66].

Some common features of the Casimir-force experiments include measurement of the force with a mechanical transducer, via its change in position or in resonant frequency; calibration with electrostatic

forces; vibration isolation; minimization and strict accounting of external forces between the objects and with surroundings, including electrostatic, magnetic and gravitational forces; measurement and control of separations with screws and piezoelectrics. Surfaces are typically gold plated; however, measurements with other metals, such as copper, and semiconductors, such as germanium and silicon, have been done. Imperfections in the materials can have a significant effect.

Most experiments are done at room temperature. At low temperatures, noise caused by refrigeration equipment becomes a serious problem; however, low temperature does reduce electron-phonon scattering in the materials, and results indicate that the Casimir effect is independent of these interactions. High temperatures are impractical due to thermal expansion of the apparatus.

Some remaining experimental issues include having a model for the frequency dependence of the permittivity, in order to compare with theory, and residual electrostatic interactions associated with surfaces not being exact equipotentials. Use of atomic force microscopy methods, with spherical or cylindrical probes, may be useful.

All of these measurements focus on a Casimir force derived from electromagnetism. There has not been a measurement of a Casimir force due to any other type of field. However, measurement of the electromagnetic Casimir force can be used to constrain models of new long-range forces due to exchange of light particles [67, 68] as well as search for deviations from Newtonian gravity.

A related experiment [69] tests the polarization of an atomic core by an electron in a high Rydberg state. Bernabéu and Tarrach [70] had applied dispersion theory to obtain a retardation correction

$$V = \frac{11\hbar e^2 \alpha}{4\pi m c r^5} \quad (8)$$

to the potential for an electron a distance  $r$  from a polarizable object with polarizability  $\alpha$ . Kelsey and Spruch [71] obtained the same correction using perturbation theory. They also derived this form by invoking the zero-point energy of the electromagnetic field [72]. These results were confirmed in a dispersion theoretic analysis by Feinberg and Sucher [73].

## 2.6 Thermal effects

The spectral density of photons at a temperature  $T$  is

$$\rho(\omega) = \frac{\hbar\omega^3}{\pi^2 c^3} \left[ n(\omega) + \frac{1}{2} \right], \quad (9)$$

where  $n(\omega) = 1/(e^{\hbar\omega/kT} - 1)$  is the thermal photon number in Bose-Einstein statistics. The  $\frac{1}{2}$  term is from virtual photons, and the limit of  $T \rightarrow 0$  yields the spectral energy density of the vacuum

$$\rho_0(\omega) = \frac{\hbar\omega^3}{2\pi^2 c^3}. \quad (10)$$

This is consistent with the requirement that the vacuum spectral density be Lorentz invariant [74]; uniform motion relative to the vacuum cannot be detected. The requirement of an  $\omega^3$  dependence follows from the force on a neutral system moving through a thermal radiation field with spectral density  $\rho$ , which is given by [75]  $\rho - \frac{\omega}{3} \frac{d\rho}{d\omega}$  and is zero for  $\rho \propto \omega^3$ .

For an accelerated observer, there is an effect; the observer sees the equivalent of a thermal bath with an effective temperature [76]  $T = \hbar a / 2\pi k c$ , with  $a$  the acceleration. If the external force on a charged object is constant, the acceleration will fluctuate as the charge interacts with the fluctuations in this apparent thermal bath of vacuum fields. The charge then radiates, which damps the motion [77].

Thermal effects for the Casimir force become important when the separation is larger than the thermal wavelength  $\hbar c / kT$ . The force between plates is then dominated by thermal photons with a

pressure of [39]

$$P = -\frac{2.4kT}{4\pi a^3}. \quad (11)$$

This has a  $a^{-3}$  dependence instead of  $a^{-4}$  and is independent of  $\hbar$ , making it no longer a quantum effect. At smaller separations, experiments need to take thermal effects into account in order to accurately evaluate the Casimir force. For finite temperature, the zero-point energy  $E_0 = \frac{1}{2} \sum_n \hbar\omega_n$  is augmented as the free energy [2]

$$\mathcal{F} = \sum_n \left[ \frac{1}{2} \hbar\omega_n + kT \ln(1 - e^{-\hbar\omega_n/kT}) \right]. \quad (12)$$

For temperatures much below  $\hbar c/4\pi ka$ , the pressure between parallel plates is [78, 39]

$$P = -\frac{\pi^2 \hbar c}{240a^4} \left[ 1 + \frac{1}{3} \left( \frac{T}{T_{\text{eff}}} \right) \right], \quad (13)$$

where  $T_{\text{eff}} \equiv \hbar c/2ak \sim 10^3 \text{K} \mu\text{m}/a$ . Thus, for separations on the order of a micron, the effective temperature is quite high and temperature effects are low. The analysis assumes that the apparatus is at thermal equilibrium; for surfaces at different temperatures, thermal photons are emitted and absorbed at different rates. For realistic materials, there is also temperature dependence through the permittivity and the permeability.

## 3 Calculations

### 3.1 Equal-time quantization

For simplicity, we present the calculation for a free massless scalar field  $\phi$ , subject to boundary conditions consistent with a chosen positioning of the plates. The Lagrangian is<sup>2</sup>

$$\mathcal{L} = \frac{1}{2} (\partial_\mu \phi)^2, \quad (14)$$

and the Hamiltonian density is

$$\mathcal{H} \equiv \partial_0 \phi \partial_0 \phi - \mathcal{L} = \frac{1}{2} (\partial_0 \phi)^2 + \frac{1}{2} (\vec{\partial} \phi)^2. \quad (15)$$

The mode expansion for the field is

$$\phi = \frac{1}{(2\pi)O^{3/2}} \int \frac{d^3 p}{\sqrt{2|\vec{p}|}} \left\{ a(\vec{p}) e^{-ip \cdot x} + a^\dagger(\vec{p}) e^{ip \cdot x} \right\}, \quad (16)$$

with the nonzero commutation relation

$$[a(\vec{p}), a^\dagger(\vec{p}')] = \delta(\vec{p} - \vec{p}'). \quad (17)$$

Without normal ordering, the vacuum expectation value of the Hamiltonian density is

$$\langle 0 | \mathcal{H} | 0 \rangle_{\text{free}} = \frac{1}{2(2\pi)^3} \int p d^3 p, \quad (18)$$

which is, of course, infinite.

---

<sup>2</sup>In this section, we use units for which  $\hbar = 1$  and  $c = 1$ .

If the field is constrained to satisfy periodic boundary conditions at parallel plates, separated a distance  $a$  and perpendicular to the  $z$  axis, the  $z$  component of momentum is constrained to be discrete

$$\phi(z+a) = \phi(z) \Rightarrow e^{ip_z a} = 1 \Rightarrow p_z = \frac{2\pi n}{a}, \quad (19)$$

with  $n$  any integer. The integral over  $p_z$  is then replaced by a sum

$$\langle 0|\mathcal{H}|0\rangle_{\text{PBC}} = \frac{2\pi}{a} \sum_n \frac{1}{2(2\pi)^3} \int E_n d^2 p_\perp = \frac{1}{2a(2\pi)^2} \sum_{n=-\infty}^{\infty} \int E_n d^2 p_\perp, \quad (20)$$

where  $E_n \equiv \sqrt{p_\perp^2 + \left(\frac{2\pi n}{a}\right)^2}$ . This density is also infinite, requiring regularization and subtraction.

To regulate, we introduce a heat-bath factor  $e^{-\lambda E_n}$  and take the limit of  $\lambda \rightarrow 0$  after computing the density and subtracting the free-space density, computed with the same regularization. The density for periodic boundary conditions is then

$$\langle 0|\mathcal{H}|0\rangle_{\text{PBC}} = \frac{1}{2a(2\pi)^2} \sum_{n=-\infty}^{\infty} \int E_n e^{-\lambda E_n} d^2 p_\perp. \quad (21)$$

The integral is readily performed in polar coordinates where the angular integral yields  $2\pi$  and a change of variable from  $p_\perp$  to  $E_n$  leaves

$$\int E_n e^{-\lambda E_n} d^2 p_\perp = 2\pi \int_{2\pi n/a}^{\infty} E_n^2 e^{-\lambda E_n} dE_n = \frac{4\pi e^{-2\lambda\pi n/a}}{\lambda^2 a^2} (a^2 + 2a\lambda n\pi + 2\lambda^2 n^2 \pi^2). \quad (22)$$

The sum over  $n$  is computed as a geometric series in  $e^{-2\lambda\pi/a}$  or derivatives of such a series, to account for leading factors of  $n$  and  $n^2$ . The final result is

$$\langle \mathcal{H} \rangle_{\text{PBC}} = \frac{3}{2\pi^2 \lambda^4} - \frac{\pi^2}{90a^4} + \frac{2\pi^4 \lambda^2}{315a^6} + \mathcal{O}(\lambda^4). \quad (23)$$

Repeating similar steps for the free-space density yields

$$\langle 0|\mathcal{H}|0\rangle_{\text{free}} = \frac{3}{2\pi^2 \lambda^4}. \quad (24)$$

Subtraction and the limit  $\lambda \rightarrow 0$  give the regulated vacuum energy density

$$\mathcal{E}_{\text{PBC}} \equiv \langle 0|\mathcal{H}|0\rangle_{\text{PBC}} - \langle 0|\mathcal{H}|0\rangle_{\text{free}} = -\frac{\pi^2}{90a^4}. \quad (25)$$

The energy per unit area between the plates is  $a\mathcal{E}_{\text{PBC}}$ , and its derivative yields the (negative of the) pressure

$$P_{\text{PBC}} = -\frac{d}{da}(a\mathcal{E}_{\text{PBC}}) = -\frac{\pi^2}{30a^4}. \quad (26)$$

If instead we impose boundary conditions were the field  $\phi$  must be zero at the plates, in analogy with the electromagnetic boundary conditions at a perfect conductor, the  $z$  component of momentum is discretized as  $p_z = n\pi/a$ . The calculation is then the same as for periodic boundary conditions, with  $a$  replaced by  $2a$  except in the step of finding the energy per unit area where  $a$  is unchanged as the separation between the plates. We then have

$$\mathcal{E}_{\text{0BC}} = -\frac{\pi^2}{90(2a)^4} \quad (27)$$

and

$$P_{\text{0BC}} = -\frac{d}{da}(a\mathcal{E}_{\text{0BC}}) = -\frac{\pi^2}{360a^4}. \quad (28)$$

These considerations are all at zero temperature. To extend to finite temperature  $T$ , we must use the free energy density for these bosons, obtained by [2] replacing  $\frac{1}{2}E_n$  with  $\frac{1}{2}E_n + kT \ln[1 - e^{-E_n/kT}]$  in Eq. (20):

$$\mathcal{F}_{\text{PBC}} = \frac{1}{2a(2\pi)^2} \sum_{n=-\infty}^{\infty} \int \{E_n + 2kT \ln[1 - e^{-E_n/kT}]\} d^2p_{\perp}. \quad (29)$$

From this we must subtract the free energy density without the periodic boundary conditions

$$\mathcal{F}_{\text{free}} = \frac{1}{2(2\pi)^3} \int \{p + 2kT \ln[1 - e^{-p/kT}]\} d^3p. \quad (30)$$

The difference of the first terms is as before, after regularization. The temperature dependent second terms do not require regularization; they contribute

$$\mathcal{F}_{\text{PBC}}^T = \frac{kT}{a(2\pi)^2} \sum_{n=-\infty}^{\infty} \int \ln[1 - e^{-E_n/kT}] d^2p_{\perp} - \frac{kT}{(2\pi)^3} \int \ln[1 - e^{-p/kT}] d^3p \quad (31)$$

To simplify this expression, use new integration variables  $x = E_n/kT$  and  $y = p/kT$ . Then, with  $d^2p_{\perp}$  replaced by  $2\pi(kT)^2 x dx$  and  $d^3p$  replaced by  $4\pi(kT)^3 y^2 dy$ , we have

$$\mathcal{F}_{\text{PBC}}^T = \frac{(kT)^3}{2\pi a} \sum_{n=-\infty}^{\infty} \int_{2\pi n/kTa}^{\infty} \ln[1 - e^{-x}] x dx - \frac{2(kT)^4}{(2\pi)^2} \int_0^{\infty} \ln[1 - e^{-y}] y^2 dy. \quad (32)$$

Given the integral representation for the zeta function

$$\zeta(s) = \frac{1}{(s-1)!} \int_0^{\infty} \frac{x^{s-1} dx}{e^x - 1} \quad (33)$$

and an integration by parts, this part of the free energy density can be rewritten as

$$\mathcal{F}_{\text{PBC}}^T = -\frac{(kT)^3}{2\pi a} \zeta(3) + 2\frac{(kT)^3}{2\pi a} \sum_{n=1}^{\infty} \int_{2\pi n/kTa}^{\infty} \ln[1 - e^{-x}] x dx + \frac{4(kT)^4}{(2\pi)^2} \zeta(4). \quad (34)$$

For low temperatures, where  $2\pi a/kT \gg 1$ , the remaining logarithm can be expanded in powers of  $e^{-x}$ . The leading contribution is of order  $e^{-2\pi n/kTa}$ . Therefore, the dominant exponential contribution is for  $n = 1$ ; the subleading contribution for  $n = 1$  is of order  $e^{-4\pi/kTa}$ , which is the same order as the leading  $n = 2$  contribution. The low temperature form of the Casimir free-energy density is then

$$\mathcal{F}_{\text{PBC}} = -\frac{\pi^2}{90a^4} - \frac{(kT)^3}{2\pi a} \zeta(3) - 2\frac{(kT)^3}{2\pi a} \left[1 + \frac{2\pi}{kTa}\right] e^{-2\pi n/kTa} + \frac{4(kT)^4}{(2\pi)^2} \zeta(4). \quad (35)$$

For a high-temperature expansion, see [2].

### 3.2 Light-front quantization

Light-front coordinates [12, 18] are the light-front time  $x^+ \equiv t - z$ , the longitudinal spatial coordinate  $x^- \equiv t + z$ , and the transverse coordinates  $\vec{x}_{\perp} = (x, y)$ . The three light-front spatial coordinates are combined as  $\underline{x} = (x^-, \vec{x}_{\perp})$ . The axes for light-front time and longitudinal space are shown in Fig. 1. The conjugate light-front energy and momentum are  $p^- \equiv E - p_z$  and  $\underline{p} = (p^+ \equiv E + p_z, \vec{p}_{\perp} \equiv (p_x, p_y))$ .

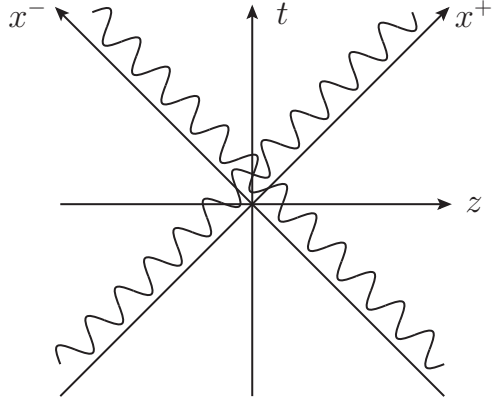


Figure 1: Light-front coordinates. The light wave along the  $x^-$  axis is everywhere at one light-front time  $x^+$ .

The scalar product of momentum and position four-vectors is  $p \cdot x = \frac{1}{2}(p^- x^- + p^+ x^+) - \vec{p}_\perp \cdot \vec{x}_\perp$ . The mass shell condition  $p^2 = m^2$  can then be reinterpreted as  $p^- = (p_\perp^2 + m^2)/p^+$ .

A calculation of the Casimir force in light-front coordinates [21] requires care with respect to the interpretation of energy and the meaning of the boundary conditions. The energy must be the ordinary equal-time energy  $E$ , not the light-front energy  $P^-$ , because the variation of  $E$  is what yields the force. The plates must be at rest in some frame rather than separated by a fixed distance in  $x^-$ ; in the latter case, the plates would be moving with the speed of light in any rest frame, which is unphysical. The correct configuration is depicted in Fig. 2. There is also the alternate possibility of plates separated in a transverse direction, which we consider in a subsequent section.

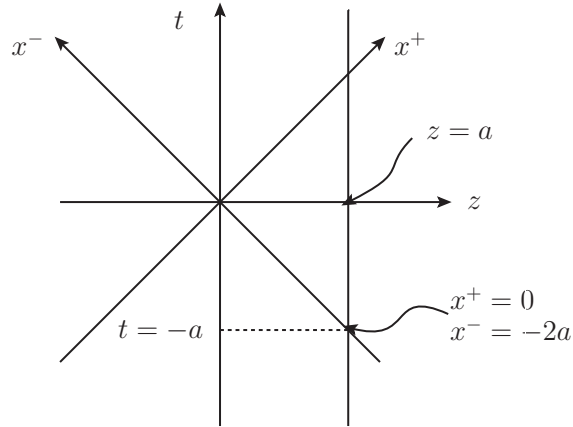


Figure 2: Parallel plates located at  $z = 0$  and  $z = a$ . The plate at  $z = a$  intersects the  $x^-$  axis at  $x^- \equiv t - z = -2a$ .

The Lagrangian for a massless scalar field is, again,

$$\mathcal{L} = \frac{1}{2}(\partial_\mu \phi)^2 = \frac{1}{2}\partial_- \phi \partial_+ \phi - \frac{1}{2}(\vec{\partial}_\perp \phi)^2, \quad (36)$$

and the light-front Hamiltonian density is

$$\mathcal{H}^- \equiv \partial_- \phi \frac{\delta \mathcal{L}}{\delta(\partial_- \phi)} - \mathcal{L} = \frac{1}{2}(\vec{\partial}_\perp \phi)^2. \quad (37)$$

We will also need the light-front longitudinal momentum density

$$\mathcal{H}^+ = \partial_- \phi \frac{\delta \mathcal{L}}{\delta(\partial_+ \phi)} = 2 \left( \frac{\partial \phi}{\partial x^-} \right)^2. \quad (38)$$

The mode expansion for the field is

$$\phi = \int_{p^+ \geq 0} \frac{d\underline{p}}{\sqrt{16\pi^3 p^+}} \left\{ a(\underline{p}) e^{-i\underline{p} \cdot x} + a^\dagger(\underline{p}) e^{i\underline{p} \cdot x} \right\}, \quad (39)$$

with the nonzero commutation relation

$$[a(\underline{p}), a^\dagger(\underline{p}')] = \delta(\underline{p} - \underline{p}') \equiv \delta(p^+ - p'^+) \delta(\vec{p}_\perp - \vec{p}'_\perp). \quad (40)$$

### 3.2.1 Longitudinal separation

For comparison with the equal-time calculation, we first consider the calculation for periodic boundary conditions consistent with plates perpendicular to the  $z$  axis. The periodicity condition is  $\phi(z + a) = \phi(z)$ , but we must translate this to light-front coordinates, where we have

$$\phi(x^+ + a, x^- - a, \vec{x}_\perp) = \phi(x^+, x^-, \vec{x}_\perp). \quad (41)$$

The discretization of the conjugate momentum  $p^+$  is then given implicitly by

$$-p^+ a/2 + p^- a/2 = 2\pi n, \quad (42)$$

with  $p^- = p_\perp^2/p^+$  and  $n$  any integer in the interval  $(-\infty, \infty)$ . The solution of this constraint, that respects the positivity of  $p^+$ , is

$$p_n^+ \equiv \frac{2\pi}{a} n + \sqrt{\left(\frac{2\pi}{a} n\right)^2 + p_\perp^2}. \quad (43)$$

The full range of  $p^+$  is recovered, with  $n = -\infty$  yielding  $p^+ = 0$  and  $n = \infty$ ,  $p^+ = \infty$ .

With  $p^+$  being discrete, the integration over  $p^+$  is replaced by a sum over  $n$

$$\int dp^+ = \int \frac{dp^+}{dn} dn \rightarrow \sum_n \frac{dp^+}{dn} = \frac{2\pi}{a} \sum_n \frac{p_n^+}{E_n}. \quad (44)$$

The mode expansion of the field is then

$$\begin{aligned} \phi(x^+ = 0) = & \frac{1}{\sqrt{2a}} \sum_n \int \frac{d^2 p_\perp}{2\pi \sqrt{E_n}} \left\{ a_n(\vec{p}_\perp) e^{-ip_n^+ x^- / 2 + i\vec{p}_\perp \cdot \vec{x}_\perp} \right. \\ & \left. + a_n^\dagger(\vec{p}_\perp) e^{ip_n^+ x^- / 2 - i\vec{p}_\perp \cdot \vec{x}_\perp} \right\}, \end{aligned} \quad (45)$$

where we define discrete annihilation operators

$$a_n(\vec{p}_\perp) = \sqrt{\left| \frac{dp^+}{dn} \right|} a(p_n^+, \vec{p}_\perp), \quad (46)$$

for which the commutation relation becomes

$$[a_n(\vec{p}_\perp), a_{n'}^\dagger((\vec{p}_\perp)')] = \delta_{nn'} \delta(\vec{p}_\perp - \vec{p}'_\perp). \quad (47)$$

The leading  $\frac{1}{\sqrt{2a}}$  factor in (45) is the normalization factor for the discrete basis functions  $e^{-ip_n^+ x^- / 2 + i\vec{p}_\perp \cdot \vec{x}_\perp}$  on the interval  $-2a < x^- < 0$ .

The physical energy density is built from a sum of the vacuum expectation values of the light-front energy and longitudinal momentum densities, which are

$$\begin{aligned}\langle 0|\mathcal{H}^-|0\rangle &= \frac{1}{4a} \sum_{n,n'} \int \frac{d^2p_\perp d^2p'_\perp}{(2\pi)^2 \sqrt{E_n E_{n'}}} \vec{p}_\perp \cdot \vec{p}'_\perp \langle 0|a_n(\vec{p}_\perp)a_{n'}^\dagger(\vec{p}'_\perp)|0\rangle \\ &= \frac{1}{4a} \sum_n \int \frac{d^2p_\perp}{(2\pi)^2 E_n} p_\perp^2\end{aligned}\quad (48)$$

and

$$\begin{aligned}\langle 0|\mathcal{H}^+|0\rangle &= \frac{2}{2a} \sum_{n,n'} \int \frac{d^2p_\perp d^2p'_\perp}{(2\pi)^2 \sqrt{E_n E_{n'}}} \frac{p_n^+ p_{n'}^+}{4} \langle 0|a_n(\vec{p}_\perp)a_{n'}^\dagger(\vec{p}'_\perp)|0\rangle \\ &= \frac{1}{4a} \sum_n \int \frac{d^2p_\perp}{(2\pi)^2 E_n} (p_n^+)^2.\end{aligned}\quad (49)$$

The energy density is one-half of the sum of these

$$\mathcal{E}_{\text{LF}} \equiv \frac{1}{2}(\langle 0|\mathcal{H}^-|0\rangle + \langle 0|\mathcal{H}^+|0\rangle) \quad (50)$$

$$= \frac{1}{8a} \sum_n \int \frac{d^2p_\perp}{(2\pi)^2 E_n} (2E_n^2 + 2\frac{2\pi}{L} n E_n), \quad (51)$$

relative to light-front coordinates. The second term is proportional to  $\sum_{n=-\infty}^{\infty} n = 0$  and therefore zero itself. We then obtain

$$\mathcal{E}_{\text{PBC}}^{\text{LF}} = \frac{1}{4a} \sum_n \int \frac{d^2p_\perp}{(2\pi)^2} E_n. \quad (52)$$

However, this is not the same as the energy density relative to equal-time coordinates, which we denote simply by  $\mathcal{E}_{\text{PBC}}$ . We must first integrate over a finite separation between the plates

$$\int_0^a dz \mathcal{E}_{\text{PBC}} = \int_{-2a}^0 dx^- \mathcal{E}_{\text{PBC}}^{\text{LF}}. \quad (53)$$

After a change of variable from  $x^-$  to  $z = (x^+ + x^-)/2$  at fixed  $x^+$  on the right hand side, this connection reduces to

$$\mathcal{E}_{\text{PBC}} = \frac{1}{a} \int_0^a 2dz \mathcal{E}_{\text{PBC}}^{\text{LF}} = 2\mathcal{E}_{\text{PBC}}^{\text{LF}}. \quad (54)$$

Thus, the energy density is

$$\mathcal{E}_{\text{PBC}} = \frac{1}{2a} \sum_n \int \frac{d^2p_\perp}{(2\pi)^2} E_n, \quad (55)$$

which is identical with the equal-time result (20).

It is regulated in the same way. The heat-bath factor is again  $e^{-\lambda E_n}$  rather than an exponentiation of  $\mathcal{P}^-$ , because the heat bath should be a rest with the plates rather than moving at the speed of light. The subtraction is also the same, because the energy density of the free-space vacuum is independent of coordinates.

The case of zero boundary conditions is easily handled, once one recognizes that the discretization of  $p_+$  in (43) corresponds directly to the quantization of  $p_z$  as  $2\pi n/a$ . The zero boundary conditions would then correspond to  $p_z = \pi n/a$  and

$$p_n^+ \equiv \frac{\pi}{a} n + \sqrt{\left(\frac{\pi}{a} n\right)^2 + p_\perp^2}. \quad (56)$$

The analysis then proceeds in the same way as for periodic boundary conditions, except that  $E_n$  is given by  $\sqrt{\left(\frac{\pi}{a} n\right)^2 + p_\perp^2}$ . As for the equal-time calculation, the zero-boundary-condition result is obtained by replacing  $a$  with  $2a$  in the energy density.

### 3.2.2 Transverse separation

For a transverse separation, again by a distance  $a$ , there is less that is peculiar about a light-front formulation. Without loss of generality, we pick  $x$  as the transverse direction. The periodicity requirement is then

$$\phi(x^+, x^-, x + a, y) = \phi(x^+, x^-, x, y). \quad (57)$$

This implies discretization in  $p_x$  to values  $p_n \equiv 2\pi n/a$ . The mode expansion becomes

$$\begin{aligned} \phi(x^+ = 0) = \frac{1}{\sqrt{a}} \sum_n \int \frac{dp^+ dp_y}{\sqrt{8\pi^2 p^+}} \{ & a_n(p^+, p_y) e^{-ip^+ x^- / 2 + ip_n x + ip_y y} \\ & + a_n^\dagger(p^+, p_y) e^{ip^+ x^- / 2 - ip_n x - ip_y y} \}, \end{aligned} \quad (58)$$

with discrete annihilation operators

$$a_n(p^+, p_y) = \sqrt{\frac{2\pi}{a}} a(p^+, p_n, p_y), \quad (59)$$

that obey the commutation relation

$$[a_n(p^+, p_y), a_{n'}^\dagger(p'^+, p'_y)] = \delta_{nn'} \delta(p^+ - p'^+) \delta(p_y - p'_y). \quad (60)$$

The leading factor  $\frac{1}{\sqrt{a}}$  represents the normalization of the wave functions  $e^{-ip^+ x^- / 2 + ip_n x + ip_y y}$  on the interval  $0 < x < a$ .

The light-front energy and longitudinal momentum densities are

$$\begin{aligned} \langle 0 | \mathcal{H}^- | 0 \rangle &= \frac{1}{2a} \sum_{nn'} \int \frac{dp^+ dp_y dp'^+ dp'_y}{8\pi^2 \sqrt{p^+ p'^+}} (p_n p_{n'} + p_y p'_y) \langle 0 | a_n(p^+, p_y) a_{n'}^\dagger(p'^+, p'_y) | 0 \rangle \\ &= \frac{1}{2a} \sum_n \int \frac{dp^+ dp_y}{8\pi^2} \frac{p_n^2 + p_y^2}{p^+} \end{aligned} \quad (61)$$

and

$$\begin{aligned} \langle 0 | \mathcal{H}^+ | 0 \rangle &= \frac{2}{a} \sum_{nn'} \int \frac{dp^+ dp_y dp'^+ dp'_y}{8\pi^2 \sqrt{p^+ p'^+}} \frac{p^+ p'^+}{4} \langle 0 | a_n(p^+, p_y) a_{n'}^\dagger(p'^+, p'_y) | 0 \rangle \\ &= \frac{1}{2a} \sum_n \int \frac{dp^+ dp_y}{8\pi^2} p^+. \end{aligned} \quad (62)$$

When summed, they yield

$$\mathcal{E}_{\text{PBC}}^{\text{LF}} = \frac{1}{2a} \sum_n \int \frac{dp^- dp^+ dp_y}{8\pi^2} \frac{p^- + p^+}{2} \delta\left(p^- - \frac{p_n^2 + p_y^2}{p^+}\right), \quad (63)$$

where the delta function enforces the mass-shell condition and can be rewritten as

$$\delta\left(p^- - \frac{p_n^2 + p_y^2}{p^+}\right) = p^+ \delta(p^2) = p^+ \delta(E^2 - E_n^2), \quad (64)$$

with  $E_n = \sqrt{\left(\frac{2\pi n}{a}\right)^2 + p_z^2 + p_y^2}$ . The integral is then trivially converted to an integral with respect to equal-time variables  $E = (p^+ + p^-)/2$  and  $p_z = (p^+ - p^-)/2$ :

$$\mathcal{E}_{\text{PBC}}^{\text{LF}} = \frac{1}{2a} \sum_n \int \frac{2dE dp_z dp_y}{8\pi^2} E(E + p_z) \frac{1}{2E_n} \delta(E - E_n). \quad (65)$$

The  $p_z$  term integrates to zero, being odd in  $p_z$ , and it is this term that would be missed if only the minus density  $\langle 0|\mathcal{H}^-|0\rangle$  was used to represent the energy; the plus contribution, which was critical in the longitudinal case, is zero in the transverse case.

We have thus found the energy density relative to light-front coordinates to be given by

$$\mathcal{E}_{\text{PBC}}^{\text{LF}} = \frac{1}{4a} \sum_n \int \frac{dp_z dp_y}{(2\pi)^2} E_n. \quad (66)$$

Just as for the longitudinal case, the energy density relative to equal-time coordinates is obtained with multiplication by two, to find

$$\mathcal{E}_{\text{PBC}} = \frac{1}{2a} \sum_{n=-\infty}^{\infty} \int \frac{dp_z dp_y}{(2\pi)^2} E_n, \quad (67)$$

which matches the usual equal-time result (20) and is of the same form as in the longitudinal case. The use of zero boundary conditions again alter the result only by changing the discretization to  $p_n = \pi n/a$ .

The free energy density in light-front coordinates is identical to the equal-time form (29), and no additional calculation is necessary to obtain the finite-temperature contributions. This happens because the discrete spectrum  $E_n$  and the Boltzmann factor  $e^{-E_n/kT}$  are the same. The direct equality of the spectra is explicit. The choice of Boltzmann factor is driven by the physics. A heat bath at temperature  $T$  should be at rest [79, 80, 81, 82]; a light-front Boltzmann factor of the form  $e^{-P^-/kT}$  would correspond to a heat bath moving with the speed of light.

### 3.2.3 Light-like boundary conditions

The first attempt to compute the Casimir force in light-front coordinates was by Lenz and Steinbacher [19]. In the longitudinal direction they applied light-like periodic boundary conditions on the scalar field  $\phi$ ,

$$\phi(x^+, x^- + a, x, y) = \phi(x^+, x^-, x, y), \quad (68)$$

and studied the vacuum expectation value of the light-front energy. For this expectation value they obtained

$$\langle \mathcal{P}^- \rangle = \frac{1}{2a} \int \frac{d^2 k_{\perp}}{(2\pi)^2} \sum_{n=0}^{\infty} \omega_n(k_{\perp}) e^{-\lambda^- 2\pi n/a - \lambda^+ \omega_n(k_{\perp})}, \quad (69)$$

with light-front energies  $\omega_n(k_{\perp}) \equiv \frac{k_{\perp}^2}{4\pi n/a}$ . The  $\lambda^{\pm}$  regulate the  $k^+ = 2\pi n/a$  and  $\omega_n$  dependencies separately. Their computation of the sum yields

$$\langle \mathcal{P}^- \rangle = \frac{1}{8\pi^2(\lambda^+ \lambda^-)^2} - \frac{1}{24\lambda^+ 2a^2} + \frac{\pi^2}{120a^4} \left( \frac{\lambda^-}{\lambda^+} \right)^2. \quad (70)$$

The regulator and separation dependence do not separate, making interpretation difficult.

For a transverse separation, their calculation for periodic boundary conditions leads to the standard result. As noted above, this success is due to the lack of a contribution from the vacuum expectation value of the longitudinal light-front momentum to the ordinary energy, allowing use of only  $\langle \mathcal{P}^- \rangle$  to give the full answer.

They also studied what happens when the longitudinal boundary condition is replaced with a boundary condition near the light front

$$\phi(x^+, x^- + a, x + sa, y) = \phi(x^+, x^-, x, y), \quad (71)$$

with  $s$  taken to approach zero. This condition can, of course, be transformed into an equivalent transverse boundary condition for any nonzero  $s$ . For such a condition, the light-front calculation yields the correct result. This approach leads naturally to consideration of modified light-front coordinates known as oblique light-front coordinates [83].

### 3.3 Oblique light-front coordinates

The application of oblique light-front coordinates to the Casimir-force problem was considered by Almeida, *et al.* [20]. The coordinates are defined as

$$\bar{x}^0 = t + z, \quad \bar{x}^3 = z, \quad \bar{x} = x, \quad \bar{y} = y, \quad (72)$$

with the chosen time coordinate  $\bar{x}^0$  equivalent to the light-front time  $x^+$ . For a massless scalar field  $\phi$ , the Lagrangian density is

$$\mathcal{L}_{\text{oblique}} = -\bar{\partial}_0\phi\bar{\partial}_3\phi - \frac{1}{2}(\bar{\partial}_\perp\phi)^2 - \frac{1}{2}(\bar{\partial}_3\phi)^2. \quad (73)$$

The mode expansion for the field is

$$\phi = \frac{1}{(2\pi)^{3/2}} \int d^2\bar{k}_\perp \int_0^\infty \frac{d\bar{k}_3}{2\bar{k}_3} \left[ e^{-i\bar{k}\cdot\bar{x}} a(\bar{k}) + e^{i\bar{k}\cdot\bar{x}} a^\dagger(\bar{k}) \right], \quad (74)$$

with  $\bar{k}$  the conjugate four-momentum,  $\bar{k} \equiv (\bar{k}_0, -\bar{k}_3, -\bar{k}_\perp)$ , and

$$\bar{k}_0 = \frac{\bar{k}_3^2 + \bar{k}_\perp^2}{2\bar{k}_3}. \quad (75)$$

The nonzero commutation relation for the creation and annihilation operators is

$$[a(\bar{k}), a^\dagger(\bar{q})] = 2\bar{k}_3\delta(\bar{k} - \bar{q}). \quad (76)$$

The Hamiltonian density is then

$$\mathcal{H} = \frac{1}{2} \int d^2\bar{k}_\perp \int \frac{d\bar{k}_3}{2\bar{k}_3} \bar{k}_0 [a(\bar{k})a^\dagger(\bar{k}) + a^\dagger(\bar{k})a(\bar{k})]. \quad (77)$$

As for the other methods, a transverse boundary condition yields the correct result and only the longitudinal boundary condition requires care. If the longitudinal condition is a simple periodicity in  $\bar{x}^3 = z$

$$\phi(\bar{x}^0, \bar{x}^3 + a, \bar{x}_\perp) = \phi(\bar{x}^0, \bar{x}^3, \bar{x}_\perp), \quad (78)$$

the plates are at rest in an inertial frame, unlike an  $x^-$  separation, because the condition is applied to the  $z$  direction. However, the correct result is not obtained; the regulator dependence and separation dependence remain entangled, just as in the light-front expression (70). The difficulty with this longitudinal condition is that the periodicity is taken at different Minkowski times [20].

To avoid this inconsistency, a different longitudinal condition is used

$$\phi(\bar{x}^0 + a, \bar{x}^3 + a, \bar{x}_\perp) = \phi(\bar{x}^0, \bar{x}^3, \bar{x}_\perp), \quad (79)$$

one that is fully equivalent to the longitudinal case in equal-time coordinates.<sup>3</sup> This condition leads to the discretization

$$\frac{\bar{k}_\perp^2 - \bar{k}_3^2}{2\bar{k}_3} = \frac{2\pi n}{a}, \quad (80)$$

with  $n = 0, \pm 1, \pm 2, \dots$ . The regulated vacuum expectation value of the Hamiltonian density is

$$\langle \mathcal{H} \rangle = \frac{1}{2a} \frac{1}{(2\pi)^2} \sum_{n=-\infty}^{\infty} \int d^2\bar{k}_\perp \int_0^\infty d\bar{k}_3 \bar{k}_0 \delta\left(\frac{\bar{k}_\perp^2 - \bar{k}_3^2}{2\bar{k}_3} - \frac{2\pi n}{a}\right) e^{-\lambda^3 \bar{k}_3 - \lambda^0 \bar{k}_0}. \quad (81)$$

---

<sup>3</sup>This is the direct inspiration for the work of Chabysheva and Hiller [21], that use of oblique coordinates is not necessary but rather that one must make the correct choice of longitudinal boundary condition.

A change of variables to  $k_3 \equiv \bar{k}_3 - E_k$  and  $\vec{k}_\perp = \vec{k}'_\perp$ , with  $E_k \equiv \sqrt{k_\perp^2 + k_3^2}$ , and use of the  $\delta$  function to perform the  $k_3$  integral, leaves

$$\langle \mathcal{H} \rangle = \frac{1}{2a} \frac{1}{(2\pi)^2} \sum_{n=-\infty}^{\infty} \int d^2 k_\perp E_k e^{\lambda^3 2\pi n/a - (\lambda^0 + \lambda^3) E_k}. \quad (82)$$

Evaluation of the sum and integral then give [20]

$$\langle \mathcal{H} \rangle = \frac{1}{4\pi^2(\lambda^3\lambda^0)^2} - \frac{1}{32\pi^2(\lambda_3)^4} + \frac{3\lambda^0}{64\pi^2(\lambda^3)^5} - \frac{3(\lambda^0)^2}{64\pi^2(\lambda^3)^6} - \frac{\pi^2}{90a^4} + \mathcal{O}\left(\frac{\lambda^2}{a^6}, \frac{1}{\lambda^4}\right). \quad (83)$$

This may differ in the regulator dependence, but this dependence now separates from the  $a$  dependence, leaving the correct  $-\pi^2/90a^4$  term as the physical contribution to the Casimir energy.

The correction for nonzero temperature  $T$  is computed from the free energy density [22]

$$\mathcal{F}_{\text{PBC}}^T = \frac{kT}{a(2\pi)^2} \sum_{n=-\infty}^{\infty} \int d^2 \bar{k}_\perp d\bar{k}_3 \ln [1 - e^{-\bar{k}_0/kT}] \delta\left(\frac{\bar{k}_\perp^2 - \bar{k}_3^2}{2\bar{k}_3} - \frac{2\pi n}{a}\right), \quad (84)$$

where, as before, the  $\delta$  function enforces the discretization imposed by the periodic boundary conditions. Use of the same change of variables and integration over the delta function reduces this expression to

$$\mathcal{F}_{\text{PBC}}^T = \frac{kT}{a(2\pi)^2} \sum_{n=-\infty}^{\infty} \int d^2 \bar{k}_\perp \ln [1 - e^{-E_k/kT}], \quad (85)$$

with  $E_k$  discretized as  $E_k = \sqrt{k_\perp^2 + \left(\frac{2\pi n}{a}\right)^2}$ . This is the same as the (unsubtracted) equal-time expression (31).

## 4 Summary

From cosmological to atomic scales, the quantum vacuum plays a significant role in our understanding of the Universe. As suggested by Davies [84], “the vacuum holds the key to a full understanding of the forces of nature.” The Casimir force is a prime example; though it can be computed from interatomic forces, it can also be represented in terms of variations in the quantum vacuum energy density.

Any system that can be analyzed with more than one coordinate system will be better understood. Here we have shown how the Casimir force, including thermal effects, can be computed in light-front quantization and that the results agree with those from equal-time quantization, including modest extensions of previous work [21] from periodic to zero boundary conditions and to finite temperature. This can be an aid to the incorporation of vacuum effects into nonperturbative light-front calculations [18], where the vacuum has traditionally been considered trivial.

The formulation of the Casimir boundary conditions in terms of light-front coordinates will have applications in the study of effective potentials between static sources. One immediately recognizes that a static source, meaning a source at rest in an inertial frame, will be moving in the light-front coordinate  $x^-$ . A light-front static source model must then accommodate a moving source. Taking the notion of static source too literally, that is fixed in  $x^-$ , would mean a source moving with the speed of light. This is the analog of the care taken here, that the parallel plates of the Casimir effect are static in an inertial frame.

# Acknowledgments

This manuscript is dedicated to the memory of Joseph Sucher (1930-2019), thesis advisor for JRH. The work by SSC and JRH was supported in part by the US Department of Energy through Contract No. DE-FG02-98ER41087 and in part by the Minnesota Supercomputing Institute of the University of Minnesota with grants of computing resources.

# References

- [1] H.B.G. Casimir, *Proc. K. Ned. Akad.* 51 (1948) 793
- [2] G. Plunium, B. Müller, W. Greiner, *Phys. Rep.* 134 (1986) 87
- [3] P.W. Milonni, *The Quantum Vacuum: An Introduction to Quantum Electrodynamics*, Academic Press, Boston, 1994
- [4] V.M. Mostepanenko, N.N. Trunov, *The Casimir Effect and its Applications*, Clarendon Press, Oxford, 1997
- [5] W. Dittrich, H. Gies, *Probing the Quantum Vacuum: Perturbative Effective Action Approach in Quantum Electrodynamics and its Applications*, Springer Tracts in Modern Physics, Vol. 166, Springer, Berlin, 2000.
- [6] K.A. Milton, *The Casimir effect: Physical manifestations of zero-point energy*, World Scientific, River Edge NJ, 2001
- [7] K.A. Milton, *J. Phys. A* 37 (2004) R209
- [8] S.K. Lamoreaux, *Phys. Rep.* 68 (2005) 201
- [9] W. Simpson, U. Leonhardt (ed.), *Forces of the Quantum Vacuum: An Introduction to Casimir Physics*, World Scientific, New Jersey, 2015
- [10] H.B.G. Casimir, *Physica* 24 (1956) 751
- [11] T.H. Boyer, *Phys. Rev.* 174 (1968) 1764
- [12] P.A.M. Dirac, *Rev. Mod. Phys.* 21 (1949) 392
- [13] S.J. Brodsky, H.-C. Pauli, S.S. Pinsky, *Phys. Rep.* 301 (1998) 299
- [14] J. Carbonell, B. Desplanques, V.A. Karmanov, J.F. Mathiot, *Phys. Rep.* 300 (1998) 215
- [15] G.A. Miller, *Prog. Part. Nucl. Phys.* 45 (2000) 83
- [16] M. Burkardt, *Adv. Nucl. Phys.* 23 (2002) 1
- [17] B.L.G. Bakker *et al.*, *Nucl. Phys. Proc. Suppl.* 251-252 (2014) 165
- [18] J.R. Hiller, *Prog. Part. Nucl. Phys.* 90 (2016) 75
- [19] F. Lenz, D. Steinbacher, *Phys. Rev. D* 67 (2003) 045010
- [20] T. Almeida, V.S. Alves, D.T. Alves, S. Perez, P.L.M. Rodrigues, *Phys. Rev. D* 87 (2013) 065028
- [21] S.S. Chabysheva, J.R. Hiller, *Phys. Rev. D* 88 (2013) 085006
- [22] P.L.M. Rodrigues, S. Perez, D.T. Alves, V.S. Alves, C.R. Silva, arXiv:1501.01190 [hep-th]
- [23] S.A. Fulling, K.A. Milton, P. Parashar, A. Romeo, K.V. Shajesh, J. Wagner, *Phys. Rev. D* 76 (2007) 025004
- [24] R.L. Jaffe, *Phys. Rev. D* 72 (2005) 021301(R)
- [25] J.N. Munday, *Physics Today* Oct (2019) 74
- [26] F. London, *Z. Phys.* 63 (1930) 245
- [27] H.B.G. Casimir, D. Polder, *Phys. Rev.* 73 (1948) 360

- [28] H.G.B. Casimir, *J. Chim. Phys.* 46 (1949) 407
- [29] W.E. Lamb, R.C. Retherford, *Phys. Rev.* 72 (1947) 241
- [30] H.A. Bethe, *Phys. Rev.* 72 (1947) 339
- [31] T.A. Welton, *Phys. Rev.* 74 (1948) 1157
- [32] R.P. Feynman, in *Quantum Theory of Fields*, R. Stoops (ed.), Wiley, New York, 1961
- [33] H.B. Callen, T.A. Welton, *Phys. Rev.* 83 (1951) 34
- [34] P.W. Milonni, *Phys. Rep.* 25 (1976) 1
- [35] As quoted by H. Rechenberg, in M. Bordag (ed), *The Casimir Effect 50 Years Later*, World Scientific, Singapore, 1999.
- [36] S. Weinberg, *Rev. Mod. Phys.* 61 (1989) 1
- [37] P. Candelas, S. Weinberg, *Nucl. Phys. B* 237 (1984) 397
- [38] M. Lachieze-Rey, J.-P. Luminet, *Phys. Rep.* 254 (1995) 135
- [39] J. Schwinger, L.L. Deraad Jr., K.A. Milton, *Ann. Phys. (N.Y.)* 115 (1978) 1
- [40] E.M. Lifshitz, *Sov. Phys. JETP* 6 (1958) 130 ; I.E. Dzyaloshinskii, E.M. Lifshitz, L.P. Pitaevskii, *Sov. Phys. Uspekhi* 4 (1961) 153
- [41] M. Born, E. Wolf, *Principles of Optics*, Pergamon Press, Oxford, 1970
- [42] J.D. Jackson, *Classical Electrodynamics*, Wiley, New York, 1999
- [43] M.E. Bowers, C.R. Hagen, *Phys. Rev. D* 59 (1998) 025007
- [44] G. Barton, *J. Phys. A* 34 (2001) 4083
- [45] O. Kenneth, I. Klick, *Phys. Rev. Lett.* 97 (2006) 160401
- [46] D.A.T. Somers, *et al.*, *Nature* 564 (2018) 386
- [47] D.J. Heizen, M.S. Feld, *Phys. Rev. Lett.* 59 (1987) 2623
- [48] K.H. Drehaage, in *Progress in Optics Vol. 12*, E. Wolf (ed.), North-Holland, Amsterdam, 1974.
- [49] G. Barton, *Proc. Roy. Soc. London A* 320 (1970) 251
- [50] R.W. Milonni, P.L. Knight, *Opt. Commun.* 9 (1973) 119
- [51] M.R. Philpott, *Chem. Phys. Lett.* 19 (1973) 435
- [52] R.G. Hulet, E.S. Hilfer, D. Kleppner, *Phys. Rev. Lett.* 55 (1985) 2137
- [53] H. Grotch, E. Kazes, *Am. J. Phys.* 45 (1997) 618
- [54] C.E. DeTar, J.F. Donoghue, *Ann. Rev. Nucl. Part. Sci.* 33 (1983) 235
- [55] K.A. Milton, *Phys. Rev. D* 22 (1980) 1441 ; *Phys. Rev. D* 22 (1980) 1444 ; *Phys. Rev. D* 27 (1983) 439
- [56] A. Chodos, C.B. Thorn, *Phys. Lett. B* 535 (1974) 359
- [57] K. Johnson, *Acta Phys. Polonica B* 6 (1975) 865
- [58] K.A. Milton, *Ann. Phys. (N.Y.)* 150 (1983) 432
- [59] P.W. Milonni, W.A. Smith, *Phys. Rev. A* 11 (1975) 814
- [60] P.W. Milonni, J.R. Ackerhalt, W.A. Smith, *Phys. Rev. Lett.* 31 (1973) 958
- [61] A. Erdélyi, *et al.*, *Higher Transcendental Functions*, Vol. 1, McGraw-Hill, New York, 1953
- [62] M.J. Sparnaay, *Physica* 24 (1958) 751
- [63] S.K. Lamoreaux, *Phys. Rev. Lett.* 78 (1997) 5
- [64] J.N. Munday, F. Capasso, V.A. Parsegian, *Nature* 457 (2009) 170
- [65] K. Clausius, *Angewandte Chemie* 56 (1943) 241

- [66] F. Diedrich, J.C. Berquist, W.M. Itano, D.J. Wineland, *Phys. Rev. Lett.* 62 (1989) 403
- [67] G. Feinberg, J. Sucher, *Phys. Rev. D* 20 (1979) 1717
- [68] V.M. Mostepanenko and I.Yu. Sokolov, *Phys. Rev. D* 47 (1993) 2882
- [69] S.R. Lundeen, in Atomic Physics 12, J. Zorn, R. Lewis (ed.), AIP, New York, 1991; E.A. Hessels, P.W. Arcuni, F.J. Deck, S.R. Lundeen, *Phys. Rev. A* 46 (1992) 2622 .
- [70] J. Bernabé, R. Tarrach, *Ann. Phys. (N.Y.)* 102 (1976) 323
- [71] E.J. Kelsey, L. Spruch, *Phys. Rev. A* 18 (1978) 15
- [72] L. Spruch, E.J. Kelsey, *Phys. Rev. A* 18 (1978) 845
- [73] G. Feinberg, J. Sucher, *Phys. Rev. A* 27 (1983) 1958 ; G. Feinberg, J. Sucher, C.K. Au, *Phys. Rep.* 180 (1989) 83
- [74] T.H. Boyer, *Phys. Rev.* 182 (1969) 1764
- [75] A. Einstein, L. Hopf, *Ann. d. Phys.* 33 (1910) 1105
- [76] W.G. Unruh, *Phys. Rev. D* 14 (1976) 870 ; P.C.W. Davies, *J. Phys. A* 8 (1975) 609
- [77] D.W. Sciama, P. Candelas, D. Deutsch, *Adv. Phys.* 30 (1981) 327
- [78] M.L. Levin, S.M. Rytov, The Theory of Thermal Equilibrium Fluctuations in Electrodynamics, Nauka, Moscow, 1967
- [79] S. Elser, A.C. Kalloniatis, *Phys. Lett. B* 375 (1996) 285
- [80] J.R. Hiller, Y. Proestos, S. Pinsky, N. Salwen, *Phys. Rev. D* 70 (2004) 065012 ; J.R. Hiller, S. Pinsky, Y. Proestos, N. Salwen, U. Trittmann, *Phys. Rev. D* 76 (2007) 045008
- [81] S. Strauss, M. Beyer, *Phys. Rev. Lett.* 101 (2008) 100402
- [82] S. Strauss, S. Mattiello, M. Beyer, *J. Phys. G* 36 (2009) 085006
- [83] H.A. Weldon, *Phys. Rev. D* 67 (2003) 085027 ; *Phys. Rev. D* 67 (2003) 128701
- [84] P.C.W. Davies, Superforce, p. 104, Simon and Schuster, New York, 1985